

Rapid Communications

The Rapid Communications section is intended for the accelerated publication of important new results. Manuscripts submitted to this section are given priority in handling in the editorial office and in production. A Rapid Communication may be no longer than $3\frac{1}{2}$ printed pages and must be accompanied by an abstract. Page proofs are sent to authors, but, because of the rapid publication schedule, publication is not delayed for receipt of corrections unless requested by the author.

Nature of the Si(111) 7×7 reconstruction

Mark J. Cardillo

Bell Laboratories, Murray Hill, New Jersey 07974

(Received 4 November 1980)

Specular scattering of an atomic He beam from a Si(111) 7×7 surface is analyzed in terms of interference in the normal momentum transfer. An average distance is derived which corresponds to the double-layer spacing. It is concluded that both the top and second double layer are exposed as a result of the reconstruction and it is shown that a large fraction of the top double layer is missing.

An analysis of He atomic-beam specular scattering is presented which directly implies the nature of the Si(111) 7×7 reconstruction. The principal result is that over a large fraction of the 7×7 unit mesh the top double layer is missing. Thus there are major changes in the atomic positions and bonding of the outermost atoms in the formation of the (7×7) surface. The area deduced for the missing double layer suggests a surface which consists of ordered arrays of large open regions (one double layer) which must interact over distances of several angstroms. Models which consider only perturbations to the ideal termination of the bulk such as buckling^{1,2} or even an array of top-layer single-atom vacancies³ (adatoms⁴) do not satisfactorily account for the data.

In Fig. 1 a scan of the normalized in-plane specular intensity is plotted versus incident angle θ_i for $\lambda = 0.57 \text{ \AA}$, with the incident beam projecting onto the [01]* direction. A series of strong oscillations separated by 5° – 10° are observed over the entire angular range. These features are interpreted in terms of interference in the normal momentum transfer $\Delta k_\perp = (4\pi/\lambda) \cos\theta_i$. These interference oscillations arise when the surface potential for the He atom is strongly corrugated. Similar observations and interpretations have been made for He scattering from the roughened Cu(100),⁵ Si(100),⁶ and GaAs(110)⁷ surfaces which also have large corrugations ($>1 \text{ \AA}$).

The following argument is made in one dimension but holds for the location of interference maxima arising for a three-dimensional surface. Specular scattering is taken to originate from the periodic flat parts of the surface potential, approximated by a hard

wall, for which the vertical spacing of the maximum and minimum is the value d_\perp . For specular scattering ($\Delta k_\parallel = 0$), an interference maximum can arise if the path-length difference for scattering from the top and bottom flat regions approaches $n\lambda$ where n is an integer. This is, of course, the same as Bragg's law, i.e., $2d_\perp \cos\theta_i = n\lambda$. A similar result for a hard wall can be obtained with the eikonal scattered-wave approximation.⁸ For the case of a one-dimensional corrugation written as $\zeta(x) = (d_\perp/2) \cos(2\pi x/a)$, the solution for specular scattering is $P_{00} = J_0^4(c)$ where J_0 is the Bessel function with the argument $c = d_\perp k_i \times \cos\theta_i$. Note that the extrema in J_0 (maxima in J_0^4) are separated by approximately π which is equivalent to Bragg's law for the separation between the maxima. Although this approximate scattering expression is too inaccurate to calculate intensities, the positions of the extrema should be properly predicted, and that is the principal concern here.

In Fig. 1 the angular positions of the maxima in $J_0^4(c)$ have been indicated by vertical arrows for the argument c with $d_\perp = 3.3 \text{ \AA}$. Ten features are assigned and nine of them are in excellent correspondence with the data. A further examination of the data reveals a fairly sharp oscillation at $\theta_i = 44^\circ$ which appears to broaden at both smaller and larger values of θ_i , suggesting beating of similar frequencies. Consequently dashed arrows are drawn which indicate the expected maxima if a second distance, $d_\perp = 2.95 \text{ \AA}$, is included. This second distance seems to account for the apparent splitting of the interference oscillations and the remaining unassigned peaks at $\theta_i = 60^\circ$ and 72° . The high order of the interference allows a precise determination of distance. At $\theta_i = 44^\circ$ a shift of

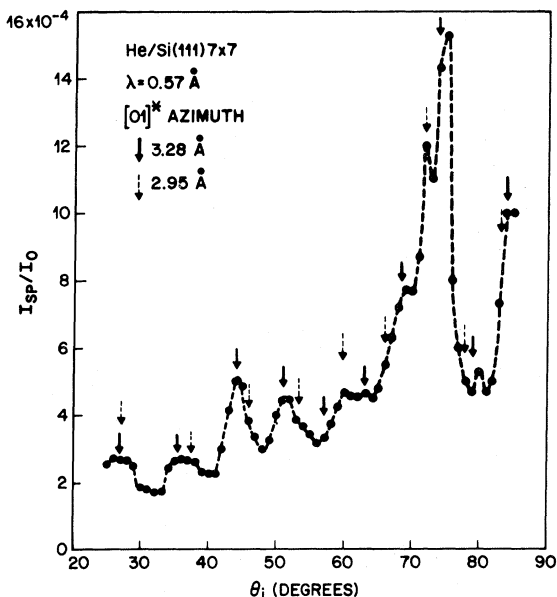


FIG. 1. Plot of the He specular intensity normalized to the incident beam versus incident angle for $\lambda = 0.57 \text{ \AA}$. The incident beam and surface normal project onto the $[01]^*$ direction. The heavy arrows indicate the position of maxima in the Bessel function J_0^4 (see text) for $d_1 = 3.28 \text{ \AA}$.

1° in assignment corresponds to $\Delta d_1 = 0.05 \text{ \AA}$. Note that the average of these two values of d_1 is 3.1 \AA , i.e., the Si(111) double-layer spacing. At $\bar{E} = 0.063 \text{ eV}$ the He atom is a completely nonpenetrating probe so that these distances derived are appropriate to the outermost exposed layer. We show below that this

result does not originate from random steps and therefore conclude that the top and second double layers are exposed within the (7×7) reconstruction of Si(111), i.e., that a part of the top double layer is missing.

In the following section the extent of the missing double layer is discussed. An estimate of the scattering cross section can be made using Si charge density at the distance of closest approach.⁹ For a repulsion of 0.063 eV the Si charge density $\rho_{\text{Si}} \sim 6 \times 10^{-4} \text{ \AA}^{-3}$. At this charge density, calculations for GaAs(110) [Ref. 9(b)] yield a distance of closest approach of 3.5 \AA with He. We assume that Si(111) has a similar exponential decay of charge density from the surface, based on similar valence binding energies, and scale the He-As radius by the ratio of the lattice constants between GaAs and Si to obtain an estimate of the He-Si interaction radius. This yields a value of 3.3 \AA . For the purpose of illustration we partition this into a Si radius of 2.3 \AA and a He radius of 1.0 \AA and draw a specular scattering trajectory for $\theta_i = 60^\circ$ in Fig. 2. There it is schematically shown that in order for a He atom to access the second double layer for $\theta_i > 60^\circ$, the extent of the exposed second-double-layer region must be at least 11 \AA . This value is insensitive to the interaction radius. Note that in Fig. 1 interference oscillations are observed for $\theta_i > 75^\circ$. The inclusion of an attractive potential may reduce this estimate slightly, however the effect will not be great as the attractive potential is weak compared to the beam energy.

The high degree of correspondence obtained in Fig. 1 for the $J_0^4(c)$ maxima, using the distances $d_1 = 3.3$

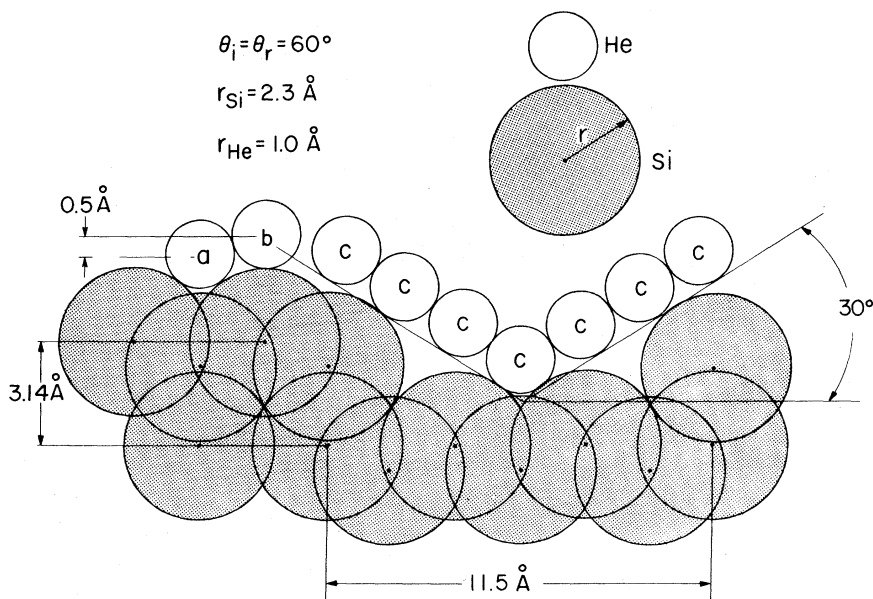


FIG. 2. Schematic drawing of a specular He trajectory at $\theta_i = 60^\circ$ which reflects from the second double layer (atoms "c"). He atoms *a* and *b* illustrate how the interaction radius determines the effective hard-wall corrugation of the undisturbed surface.

and 2.9 \AA , have been obtained without including the effect of an attractive potential. This will occur when the dimensions of the vertically interfering regions are considerably larger than the range of the attractive potential, so that the interference is the same as if it occurred in vacuum. We take an effective range of $\sim 2 \text{ \AA}$ for the attractive potential. Adding 2 \AA to the He + Si cross section yields an exposed region of $> 80 \text{ \AA}^2$.

The fit in Fig. 1, obtained without an attractive potential, suggests the possibility that these oscillations are due to random steps. The following argument shows that this is not the case. The crystal employed was cut to within $\frac{1}{2}^\circ$ of the (111) face which should yield a minimum average width of 360 \AA for the terraces between steps due to misorientation. Recent studies have shown that both "flat" 7×7 and vicinally cut surfaces tend towards very large terrace regions between steps ($\geq 1000 \text{ \AA}$) even at the cost of creating steps of much more than one double layer in height.^{10,11} Thus we expect the terrace widths to be no less than that due to misorientation (360 \AA). These minimum terrace widths are to be contrasted with what can be observed with the resolution limitations of the detector of the molecular-beam apparatus. The effective detector acceptance is $\sim 1.0^\circ$ which corresponds to $\Delta k_{\parallel} \sim 9 \times 10^{-2} \text{ \AA}^{-1}$ and therefore to distances across the crystal of $\sim 70 \text{ \AA}$. Although correlations between features on the crystal spaced up to $\sim 150 \text{ \AA}$ apart can probably be observed, the detector resolution falls far short of seeing the effect of steps spaced 360 \AA apart. The analysis of closely spaced random steps on Cu(100) (Ref. 5) gives essentially the same result and specifically confirms the conclusion here that the interference comes from within the 7×7 unit mesh.

Neither the Lander vacancy³ nor perturbation models, such as buckling or charge-density waves, can account for the major aspect of the (7×7) reconstruction shown here, namely, the absence of the top double layer over a large fraction of the unit mesh. An interesting prospect is the occurrence of large shallow triangular patches formed in a manner analogous to the formation of shallow triangular pits by oxidation.¹² Examples of these proposed flat-bottomed triangular regions are illustrated in Fig. 3 along with a drawing of the Lander vacancy model. The model essentially consists of an array of steps which intersect so as to form a 7×7 mesh. The step edges are three-bonded atoms with half-filled orbitals which interact to stabilize the surface.

The Lander model, schematically shown in Fig. 3(a), serves to illustrate the idea of a strong relaxation energy around the open region which returns more energy than the cost of a vacancy. In this case the relaxation energy was assumed to be benzenelike electronic delocalization as suggested by the shaded areas of Fig. 3(a). The analysis presented here, how-

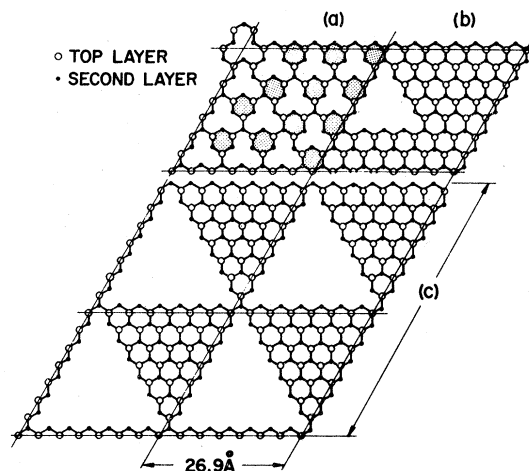


FIG. 3. Schematic drawing of the top double layer for the (7×7) unit mesh for (a) Lander vacancy model (Ref. 3), (b) minimum triangular region required to satisfy the data, and (c) model of "strongly interacting" triangular regions each occupying half of the (7×7) unit mesh.

ever, requires more equal regions of top- and second-layer exposure. Consequently, the idea of a strong relaxation around a small region becomes less significant. A larger open region, such as that drawn in Fig. 3(b) is necessary and possibly adequate for explaining the interference pattern of Fig. 1. If a vacant region of the size shown in Fig. 3(b) is formed, it would seem that either the thermal etching would continue or that the unit mesh be reduced to a 5×5 . In Fig. 3(c) the etched flat regions have been increased in area until they occupy half the 7×7 unit mesh. At this size the remaining double-layer regions can be thought of as strongly interacting with each other.

The interpretation of the two distances which differ by 0.3 \AA is not clear. It may be related to the natural He potential corrugation for one of the double layers that remains. The large He repulsive cross section ($r_{\text{Si}} + r_{\text{He}} > 3 \text{ \AA}$) will substantially reduce the nuclear corrugation of the double layer. As illustrated in Fig. 2, drawing spheres for which $r_{\text{Si}} + r_{\text{He}} \sim 3.3 \text{ \AA}$ suggests a hard-wall corrugation of $\sim 0.5 \text{ \AA}$ which would be reduced by smoothing of the cusped region. A more detailed study is required to clarify this point.

McRae has similarly analyzed low-energy electron diffraction (LEED) patterns of the hydrogenated Si(111) (7×7) surface.¹³ He concludes that the surface consists of an ordered array of large irregular hexagonal islands resembling the model proposed here. We note that Phillips¹⁴ also proposed that a "rough surface" exists based on stress relief for the Si(111) and Ge(111)Sn (7×7) surfaces. These proposals are consistent with the principal conclusion reached here.

In summary, a specular intensity scan from the Si(111) 7×7 surface has been analyzed in terms of Δk_{\perp} interference and the double-layer spacing has been obtained. For the nonpenetrating He atom this means that the third layer is exposed. A simple trajectory argument and the observation that the interference can be qualitatively fit without an attractive potential require that the exposed regions amount to a large fraction ($\sim \frac{1}{2}$) of the unit mesh. A model of triangular etched regions is presented for the purpose of illustrating the implications of this

result. Studies at other wavelengths and computation of complete diffraction spectra will be required for a detailed model. However the nature of the reconstruction seems clear from these results and it is significantly different from any previous proposal.

ACKNOWLEDGMENT

The author acknowledges the collaboration of G. E. Becker in obtaining the data.

¹D. J. Chadi *et al.*, Phys. Rev. Lett. **44**, 799 (1980).

²J. D. Levine, S. H. McFarlane, and P. Mark, Phys. Rev. B **16**, 5415 (1977).

³J. J. Lander, in *Progress in Solid State Chemistry*, edited by H. Reiss (Pergamon, Oxford, 1965), Vol. 2.

⁴W. A. Harrison, Surf. Sci. **55**, 1 (1976).

⁵J. Lapujoulade and Y. Lejay, J. Phys. (Paris) Lett. **38**, 303 (1977).

⁶M. J. Cardillo and G. E. Becker, Phys. Rev. B **21**, 1497 (1980).

⁷M. J. Cardillo, G. E. Becker, S. J. Sibener, and D. R. Miller, Surf. Sci. (in press).

⁸U. Garibaldi, A. C. Levi, R. Spadacini, and G. E. Tommei, Surf. Sci. **48**, 649 (1975).

⁹(a) N. Esbjerg and J. K. Nørskov, Phys. Rev. Lett. **45**, 807 (1980). (b) R. Laughlin (unpublished).

¹⁰J. E. Rowe and Y. Chabal (unpublished).

¹¹N. Osakabe, K. Yagi, and G. Honjo, Jpn. J. Appl. Phys. **19**, L309 (1980).

¹²H. F. Dylla, J. G. King, and M. J. Cardillo, Surf. Sci. **74**, 141 (1978).

¹³E. G. McRae and C. Caldwell (unpublished).

¹⁴J. C. Phillips, Phys. Rev. Lett. **45**, 906 (1980).